Optimization of parameters for fibre laser cutting of a 10 mm stainless steel plate

C Wandera[1]* and **V Kujanpää**[1,2]
[1] LUT Mechanical, Lappeenranta University of Technology, Lappeenranta, Finland
[2] VTT The Technical Research Centre of Finland, Lappeenranta, Finland

The manuscript was received on 15 February 2010 and was accepted after revision for publication on 15 July 2010.

DOI: 10.1177/2041297510394078

Abstract: Optimization of the fibre laser cutting parameters for attainment of high cut edge quality in 10 mm stainless steel plate was demonstrated in this study. The tested process parameters included cutting speed, focal position, and focal length. Optimization of these process parameters enhances the melt removal from the cut kerf so as to prevent the undesired dross adherence on the lower cut edge or even incomplete penetration of the workpiece when the incident intensity is not sufficient to penetrate the workpiece. Dross-free cut edges with lower surface roughness and lower deviation of cut edge squareness could be achieved by reducing the cutting speed from the maximum achievable value, using the longer focal length lens for focusing the laser beam, and with focal position located on the bottom workpiece surface. These conditions enhance a high melt removal rate resulting in a high cut edge quality.

Keywords: cut edge quality, laser cutting, thick-section, stainless steel, fibre laser

1 INTRODUCTION

Cutting of steel using laser is widely performed in industry today. Manufacturers using laser cutting in their production are particularly interested in attainment of high cut quality so that rework of cut pieces can be eliminated, high cutting speeds for maximization of productivity, and cutting reproducibility. Consequently, economical criteria affecting the choice of a suitable laser system for a particular laser cutting application are now gaining much importance. Increased process efficiency, quality, and flexibility help to reduce costs. The carbon dioxide (CO_2) laser is currently the industrial workhorse for laser cutting of metal from thin- to thick-section and the solid-state Nd:YAG laser is the laser of choice for thin-section high precision metal cutting [**1**]. The advent of the high-power fibre laser – operating at near infrared spectral range (1060–1080 nm) and having a unique combination of high power, high beam quality, and high wall plug efficiency – is expected to steer the application of solid-state lasers to the field of thick-section metal cutting which has been largely dominated by the CO_2 laser [**2**, **3**, **4**].

In the cutting of medium-section stainless steel (1–6 mm) using the ytterbium fibre laser and the CO_2 laser, higher cutting speeds have been achieved with the fibre laser than with the CO_2 laser but the CO_2 laser cut quality was better than that of the fibre laser [**5**]. The poor cut edge quality obtained in inert gas assisted laser cutting of thick-section stainless steel cutting using the high brightness fibre laser results from the difficulty in obtaining full melt ejection through the narrow thick-section cut kerfs [**6**, **7**, **8**]. Himmer *et al.* compared the cutting quality and cutting performance of the CO_2 laser and fibre laser beam sources in cutting of 10–20 mm stainless steel EN 1.4301 and reported that the cut edge quality for both laser sources was sufficient but the single mode and multimode fibre lasers in the kilowatt range increased the cutting speed [**9**]. The laser power requirement for cutting of a steel workpiece at a given cutting speed using the fibre laser is lower than that for the CO_2 laser [**10**]. The poor cut edge quality obtained in the fibre laser cutting, especially at larger workpiece thickness, is reportedly influenced by the fibre laser absorption mechanism, which is different from the absorption

*Corresponding author: LUT Mechanical, Lappeenranta University of Technology, Tuotantokatu 2, Lappeenranta, 53850, Finland.
email: cathywandera@yahoo.com

mechanism in CO_2 laser cutting owing to the different wavelengths [**11**, **12**]. The increased cutting speed advantage of fibre laser cutting of metal is mainly achieved in thin-section cutting (up to about 2 mm) and falls as workpiece thickness increases towards the medium-section (2–6 mm) and thick-section (above 6 mm). The absorptivity of the fibre laser radiation reaches a distinct maximum in the range of small sheet thickness but monotonically decreases with the sheet thickness while the absorptivity of the CO_2 laser radiation continuously grows with sheet thickness and the maximum absorptivity is attained with larger sheet thicknesses [**13**].

The maximum achievable cutting speed for a given power level and the resulting cut edge quality are governed by the process parameters including laser power, focal length of focusing lens, focal position relative to workpiece surface, type and pressure of assist gas, nozzle diameter, and nozzle stand-off distance. Different cut quality regions can be defined for different combinations of laser power and cutting speed such that optimum cut quality may be achieved with a cutting speed that is lower than the maximum cutting speed achievable with a given laser power [**14**]. Optimization of the process parameters enhances the melt removal from the cut kerf so as to prevent the undesired dross adherence on the lower cut edge or even incomplete penetration of the workpiece when the incident intensity is not sufficient to penetrate the workpiece. Lugan *et al.* investigated the cut edge quality for the CO_2 laser cutting of laser grade, mild and C-Mn steels of 6 and 12 mm thickness and reported that silicon has a positive effect on surface roughness and a negative effect on edge squareness. They also reported that an industrial survey of cutting capability trials carried out in a series of laser cutting jobshops in the United Kingdom showed a high consistency in laser cut quality between different operators, jobshops and laser cutting systems [**15**]. Olsen *et al.* presented an approach developed for laser cutting with high brightness and short wavelength lasers in which multibeam patterns are applied to control the melt flow out of the cut kerf for improved cut quality in metal cutting. The approach involves splitting up the beams from two single mode fibre lasers and combining the beams into a pattern in the cut kerf whereby the melt beam and the melt ejection beams are positioned relatively to each other [**16**].

This paper describes the particular aspects that are essential for the optimization of the fibre laser cutting process parameters for the cutting of a 10 mm stainless steel plate. The tested process parameters included cutting speed, focal position relative to the workpiece top surface, and focal length of the focusing lens. Optimization of these process parameters enables improvement of the cut edge quality by minimizing dross adherence on the lower cut edge, minimizing the cut surface roughness, and minimizing the cut edge squareness deviation.

2 EXPERIMENTAL PROCEDURE

2.1 Material and test environment

The laser beam was generated by a solid-state ytterbium fibre laser (IPG YLR-5000) delivering maximum output power of 5 kW with a nominal BPP of 5.2 mm.mrad and the laser beam was transferred to the cutting head via a 150 μm diameter optical fibre. A coaxial conical nozzle of 2.5 mm diameter was used to deliver the nitrogen assist gas jet with pressure of 20 bar. The workpiece was 10 mm thick austenitic stainless steel AISI 304 (EN 1.4301) plate with typical chemical composition given in Table 1. The surface roughness measurement was performed according to ISO standard using a Mitutoyo stylus instrument (SurfTest SJ-201 Ver3.10) with a cut-off length of 2.5 mm and total measurement length of 7.5 mm.

2.2 Laser cutting tests

Cutting of the 10 mm stainless steel plate was performed using 4 kW laser power. The process parameters that were investigated for optimization in this study included the cutting speed, focal position, and focal length such that a full factorial experiment corresponding to $4 \times 3 \times 2 = 24$ test trials was designed as given in Fig. 1. The influences of the assist gas pressure, nozzle diameter, and nozzle stand-off distance were examined in the previous experimental work conducted by the authors [**18**]. Consequently, an

Table 1 Chemical composition of workpiece material [**17**]

Stainless steel	AISI 304	(EN 1.4301)		
Element	C	Cr	Ni	Fe
Content (wt-%)	0.04	18.1	8.3	Bal.

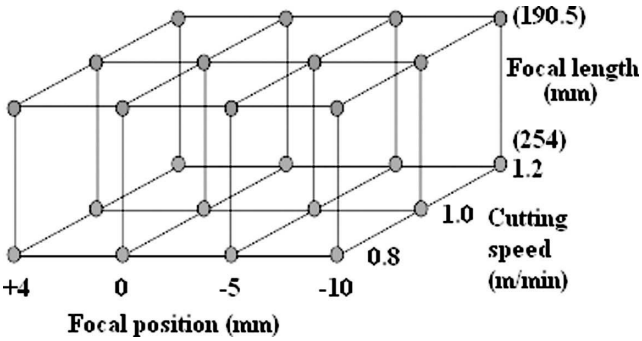

Fig. 1 Design of the experiment

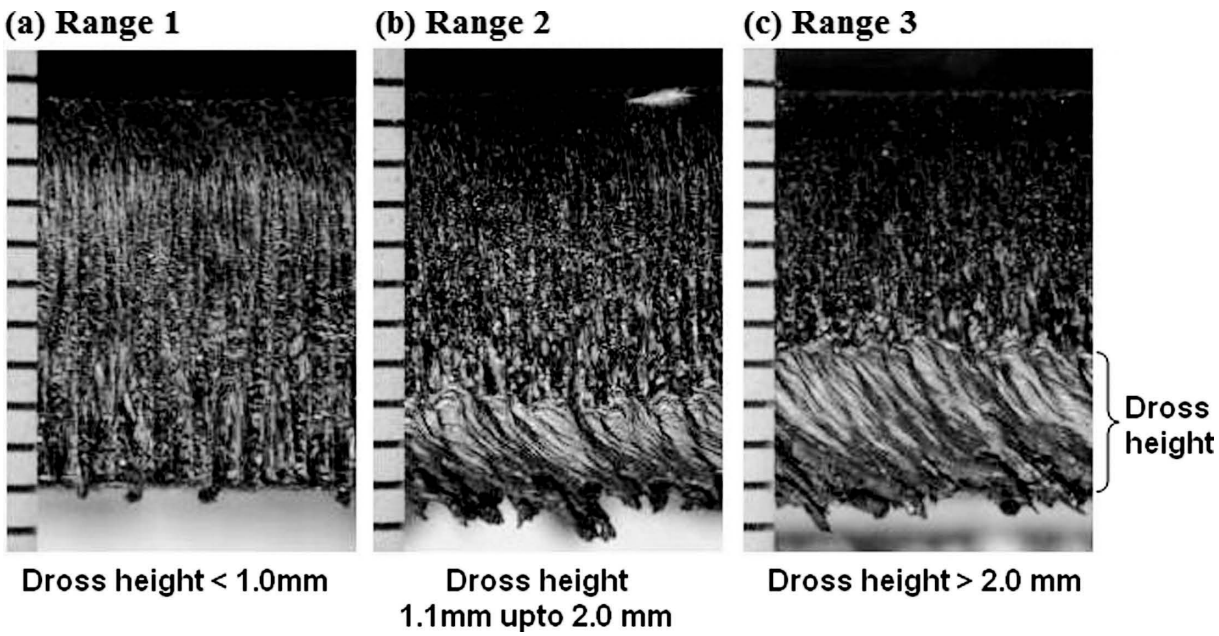

Fig. 2 Classification of dross attachment (ranges 1–3)

assist gas (nitrogen) pressure of 20 bar, nozzle diameter of 2.5 mm, and nozzle stand-off distance of 0.7 mm were chosen as constant factors in this experimental investigation.

2.3 Evaluation of cut edge quality

Evaluation of the cut edge quality from the test trials was based on the visual inspection of the dross attachment to the lower cut edge and measurement of the dross height, measurement of the cut surface roughness (R_z), and measurement of the squareness deviation of the cut edge. These were used as output factors that define the cut edge quality with the condition that the smallest value of each output factor corresponds to the best cut edge quality. Cut edge squareness deviation and cut surface roughness were categorized according to the ranges given in the standard for classification of thermal cuts, SFS EN ISO 9013: 2002, by the European Committee for Standardization [**19**]. The dross attachment was measured in terms of the height of the adherent dross that was firmly attached to the lower cut edge (see Fig. 2). Dross attachment was then evaluated according to the ranges defined by the authors as follows: range 1 (no dross) – dross height less than 1.0 mm; range 2 (little dross) – dross height from 1.1 mm to 2.0 mm; and range 3 (much dross) – dross height greater than 2.0 mm. A point system – based on the ranges for the cut edge squareness (1–5), surface roughness (1–4), and the dross attachment (1–3) – was used to evaluate the process parameters for optimum cut edge quality. The values of the ranges of the dross attachment from range 1–3, cut edge squareness deviation from range 1–5 and surface roughness from range 1–4 for the 10 mm workpiece thickness are given in Table 2. The values of the ranges of the cut edge squareness deviation and surface roughness were obtained using the formulas given in the standard for classification of thermal cuts (SFS EN ISO 9013: 2002).

Table 2 Cut quality classification for 10 mm workpiece thickness [**19**]

Range	Cut thickness with attached dross (mm)	Squareness deviation (mm)	Surface roughness (μm)
1	< 1.0 mm	0.08	16
2	1.1–2.0 mm	0.22	48
3	> 2.0 mm	0.50	82
4	–	1.00	128
5	–	1.55	–

3 RESULTS

The optimization of the laser cutting parameters for the cutting of a 10 mm stainless steel workpiece using the high power fibre laser has been demonstrated in the experiments. The laser cut edge quality is defined by the dross attachment on the lower cut edge, cut surface roughness, and cut edge squareness deviation. The size of the cut kerf is also an essential factor when considering thick-section metal laser cutting because of its influence on the rate of melt removal from the cut kerf.

3.1 Kerf width

The width of the cut kerf influences the melt removal rate in thick-section metal cutting and affects the quality of the resulting cut edge. Figure 3 presents the top kerf width for different focal length, focal position, and cutting speed. The longer focal length and defocus focal position result in a wider beam size on the workpiece surface and consequently a wider cut kerf size, which enhances the melt removal rate resulting in dross-free cut edges. The larger cut kerfs are especially important in thick-section stainless steel cutting using an inert assist gas jet because of the increased amount of the high viscosity melt with increase in workpiece thickness.

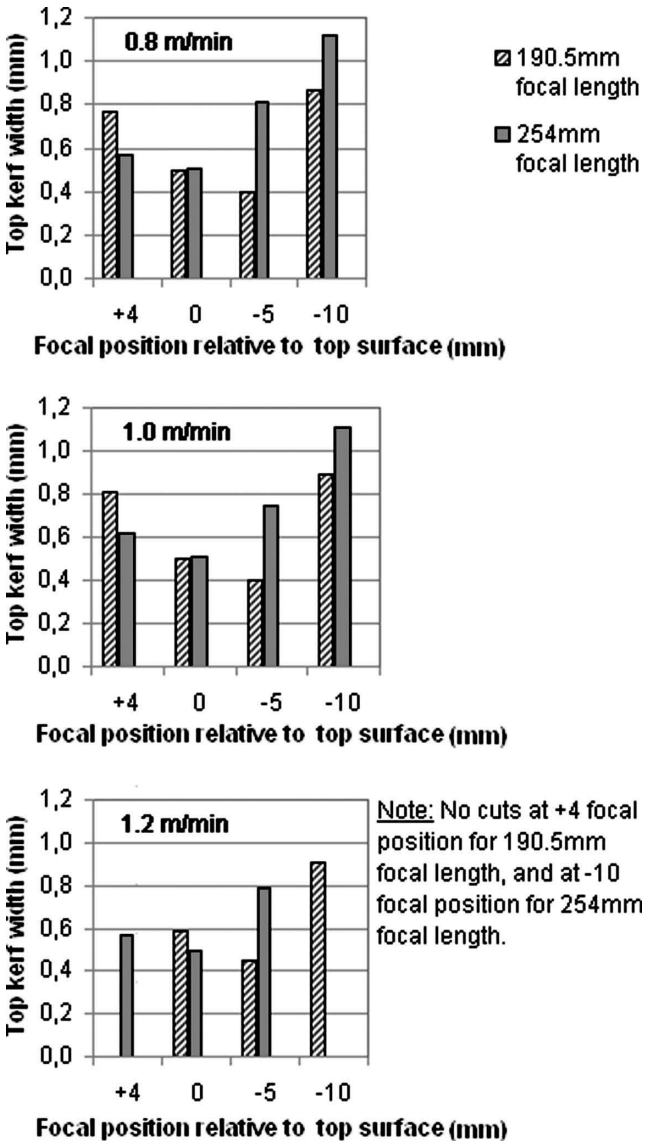

Fig. 3 Top kerf width for different focal positions

3.2 Dross attachment

The dross attachment with focal position for different cutting speeds and focal length is presented in Fig. 4. There was a decrease in the dross attachment on the lower cut edge when the focal position was located inside the workpiece. A small reduction in dross attachment with increase in cutting speed was also observed indicating that there is an optimum cutting speed that prevents dross attachment on the lower cut edge.

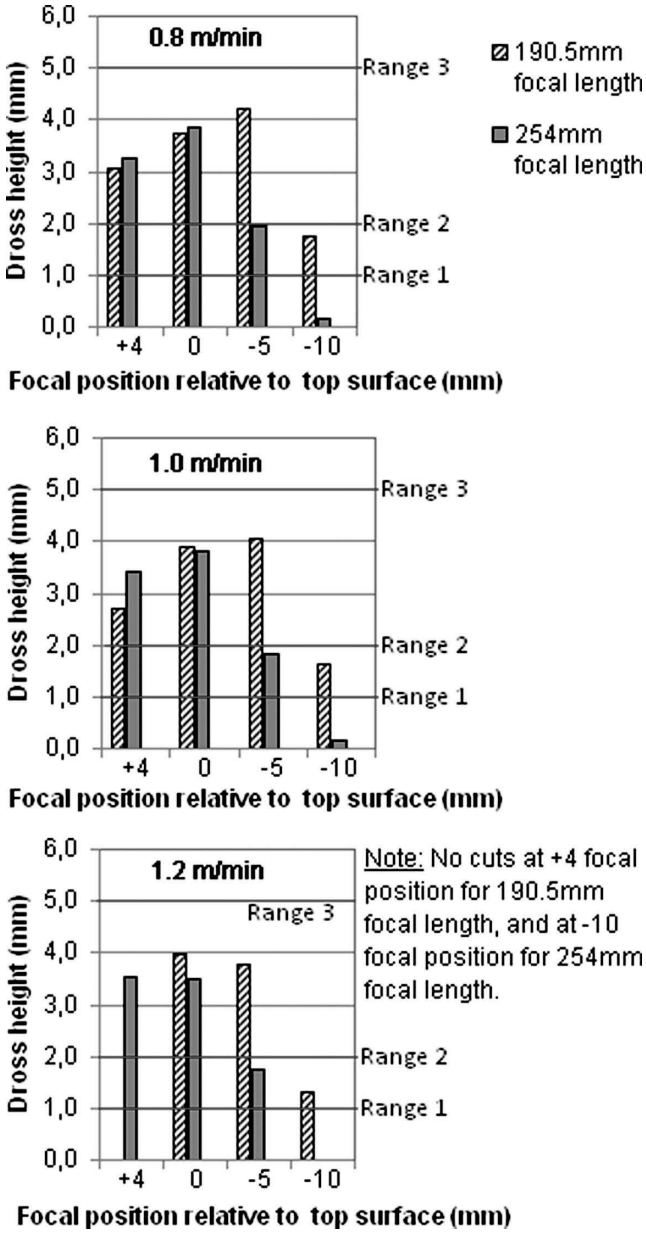

Fig. 4 Dross attachment for different focal positions (classification according to Fig. 2)

3.3 Cut surface roughness

The variation of cut surface roughness with focal position for different cutting speeds and focal length is presented in Fig. 5. There was a reduction in cut surface roughness R_z with focal position located inside the workpiece with lower surface roughness being achieved with the longer focal length of 254 mm. Using an analysis of variance shown in Table 3, it was found that the effects of cutting speed and focal position on the surface roughness were statistically significant when the focal length of 190.5 mm was used indicating that the surface roughness varies with cutting speed and focal position. The effects of cutting speed and focal position were not statistically significant when the longer focal length of 254 mm was used.

3.4 Cut edge squareness deviation

The cut edge squareness deviation with focal position for different cutting speeds is presented in Fig. 6. The cut edge squareness deviation u (determined in standard [**19**]) is notably lower for the cut edges produced with the 254 mm focal length lens than for the 190.5 mm focal length lens.

3.5 Optimum cutting parameters

Figure 7 presents the evaluation of the laser cut edge quality using points; the best cut edge quality is the one with the lowest quality points. The best cut edge quality in this study (see Fig. 8) had six quality points out of the maximum of 12. This dross-free cut edge with lower surface roughness and lower cut edge squareness deviation was achieved with the 254 mm focal length, cutting speed of 1.0 m/min, and focal position located on the bottom workpiece surface, i.e. 10 mm below the workpiece top surface.

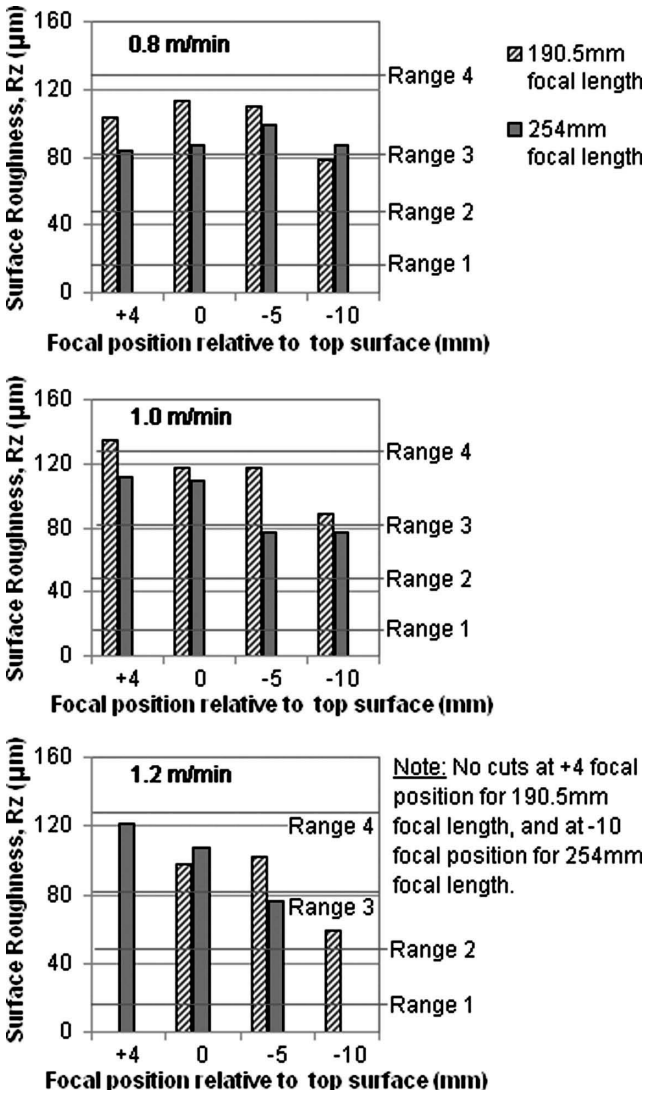

Fig. 5 Surface roughness for different focal positions.

Table 3 ANOVA: two-factor without replication

(a) Focal length of 190.5 mm

Source of variation	Sum of squares	d_f	Mean Square	F-value	P-value	F crit
Cutting speed	741.79	2	370.90	26.95	0.0048	6.9443
Focal position	2335.69	2	1167.84	84.87	0.0005	6.9443
Error	55.04	4	13.76			
Total	3132.52	8				

(b) Focal length of 254 mm

Source of variation	Sum of squares	d_f	Mean square	F-Value	P-value	F crit
Cutting speed	233.22	2	116.61	0.40	0.6929	6.9443
Focal position	762.72	2	381.36	1.32	0.3635	6.9443
Error	1158.18	4	289.55			
Total	2154.12	8				

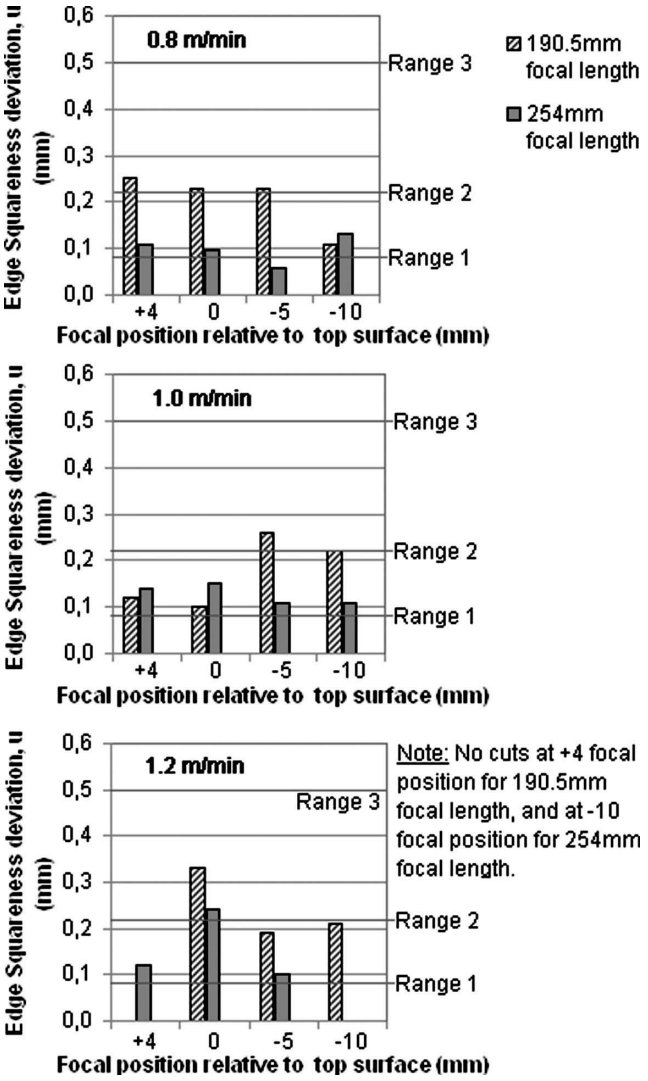

Fig. 6 Cut edge squareness deviation vs focal position

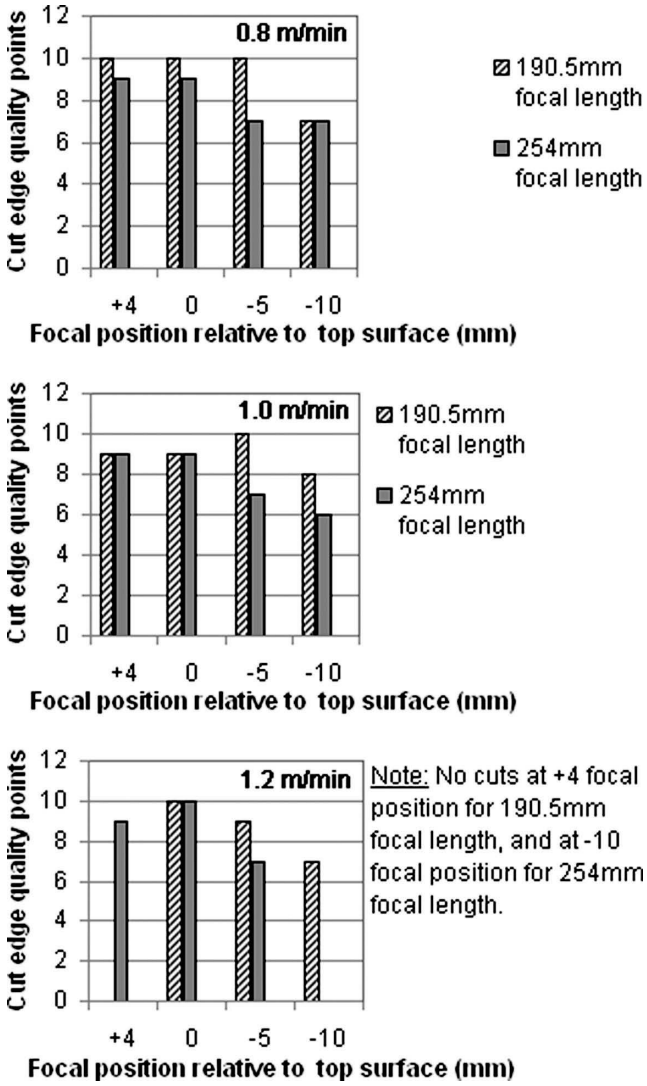

Fig. 7 Evaluation of cut edge quality

4 DISCUSSION

The focal position determines the location of the minimum focused spot size on the workpiece so that it influences both the surface power intensity necessary for penetration of the workpiece as well as the size of the cut kerf which affects the rate of melt removal from the cut kerf. Defocus focal positions – i.e. focus below workpiece top surface – are essential for thick-section metal cutting using the fibre laser as long as the power intensity at the workpiece top surface is sufficient to obtain complete penetration of the workpiece. The dross attachment on the lower cut edge and cut surface roughness are influenced by the melt removal mechanism in the narrow thick-section laser cut kerf so that resolidification of dross on the cut edge results in a higher surface roughness. The lower section of the cut edge is rougher than the upper section owing to the melt build-up at the lower cut section resulting in inefficient melt removal. Efficient melt removal is obtained when the focal position is located below the workpiece top surface because of the wider cut kerf that is created with these focal positions (see Fig. 3). Furthermore, the conduction power loss from the cutting zone to the substrate material reduces with increase in cutting speed. Therefore, the cutting speed has to be optimized for the cutting of a given workpiece thickness with a particular laser power so that the high temperature gradient at high cutting speed increases the melt fluidity for better melt removal resulting in dross-free cut edges.

When the incident laser beam is focused onto the workpiece, the beam converges towards a minimum beam waist (focused spot size) and then diverges away from this minimum beam waist. The power intensity is highest at the minimum beam waist and then decreases as the beam size grows. The beam diameter D_z at any distance along the beam path, z, from the minimum focused spot size is given by equation (1).

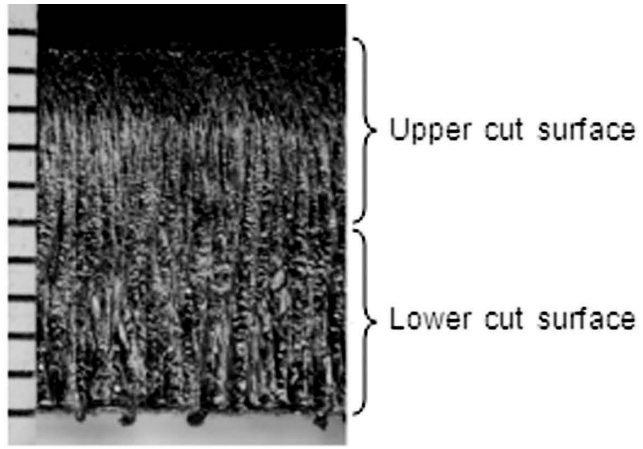

(a) Cut edge

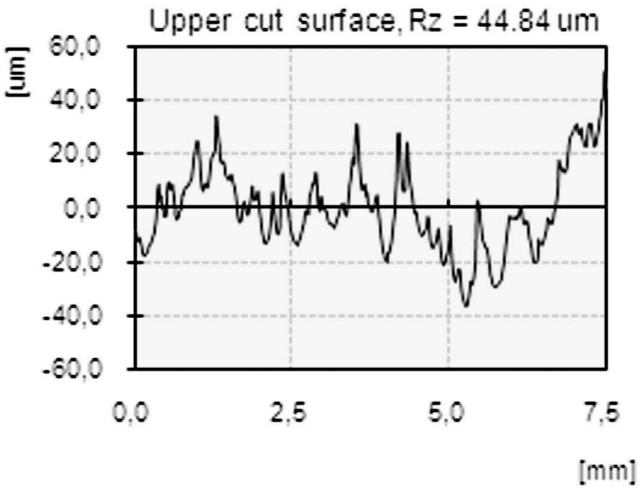

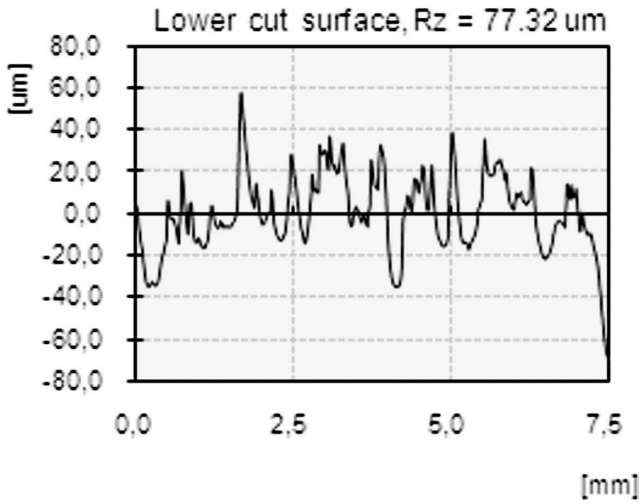

(b) Measured roughness profile

Fig. 8 Optimum cut edge quality (1.0 m/min, −10 focal position, and 254 mm focal length)

The minimum beam waist is represented by d_f; z is the distance from the minimum beam waist along the beam path; λ is wave length; M^2 and BPP are beam quality of laser beam [**20**].

$$D_Z = d_f \left\{ 1 + \left[\frac{(4M^2 \lambda z)}{(\pi d_f^2)} \right]^2 \right\}^{1/2} \tag{1}$$

But

$$\text{BPP} = \frac{\lambda}{\pi} M^2 \tag{2}$$

Therefore

$$D_Z = d_f \left\{ 1 + \left[\frac{(4z)}{(d_f^2)} \text{BPP} \right]^2 \right\}^{1/2} \tag{3}$$

Using equation (3) and the cutting conditions used in this experimental study, the fibre laser beam size on the workpiece top surface and the corresponding incident power intensity on the workpiece top surface for different focal positions are estimated and presented in Figs 9 and 10 respectively. The highest incident power intensity necessary for penetration of the workpiece at the highest cutting speed is achieved when the focal position is located at the workpiece top surface; however, the optimum focal position for dross prevention should be located inside the workpiece. When the focal position is located in the lower half section of the workpiece thickness, the incident power intensity on the workpiece top surface falls by more than half the value for focal position located on

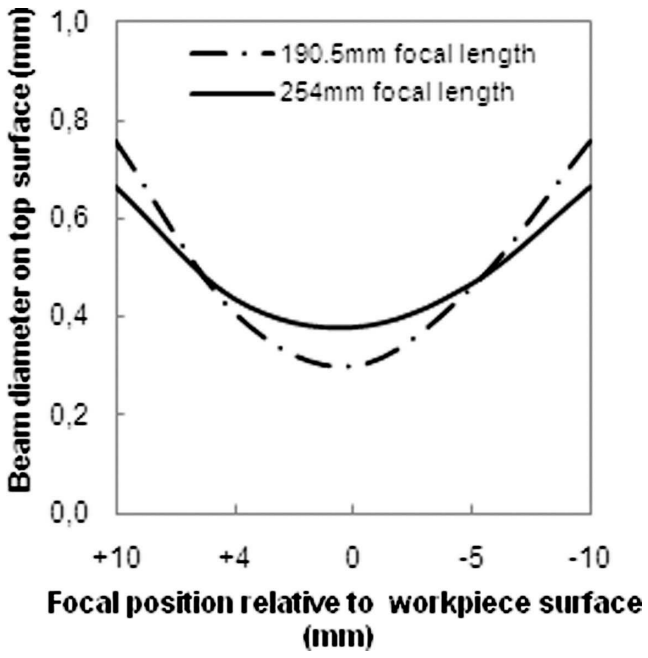

Fig. 9 Beam diameter on workpiece top surface vs focal position

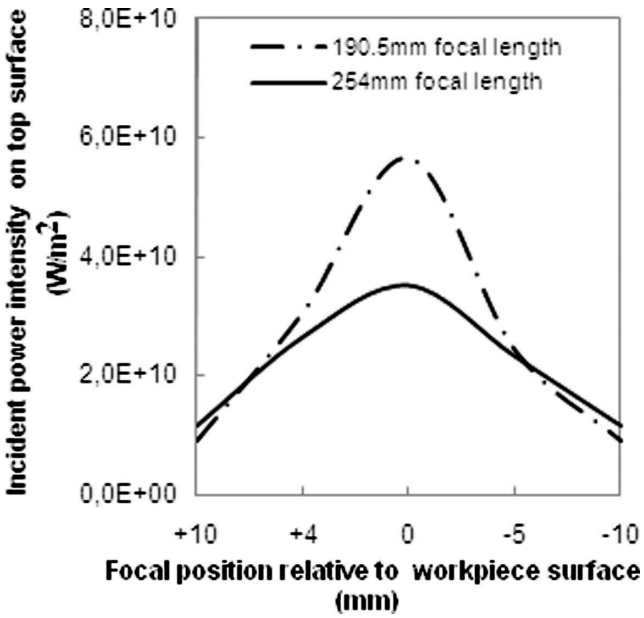

Fig. 10 Incident power intensity on workpiece top surface vs focal position

the workpiece top surface. Optimum laser cut edge quality of the 10 mm stainless steel plate using the fibre laser was obtained in this study when the cutting was performed with the focal position located on the lower surface of the workpiece as long as complete workpiece penetration could be achieved at the applied cutting speed. These defocus focal positions enable a wider cut kerf to be obtained on the workpiece surface so that a higher amount of the assist gas can enter the cut kerf and enhance the melt removal rate.

Compared to the CO_2 laser radiation, the more energetic photons of the 1.06 μm fibre laser radiation are absorbed by a greater number of bound electrons in the metal, resulting in a fall in the reflectivity and an increase in the absorptivity of the surface. The penetration of the incident laser beam into the workpiece is a function of the laser beam focusability and the depth of focus (DOF) – the distance either side of the minimum beam waist (focused spot size d_f) over which the beam diameter grows by 5 per cent – is given by equation (4) [**20**]

$$\text{DOF} = \pm 0.08\pi \frac{d_f^2}{M^2 \lambda} \tag{4}$$

Equation (4) shows that a high quality fibre laser beam having a shorter wavelength than the CO_2 laser beam would give a larger depth of focus than a CO_2 laser beam of similar beam quality when similar focusing optics is used. Consequently, this would increase the optimum penetration depth of the fibre laser and benefit the processing of thick-section metal workpieces. Additionally, the use of a longer focal length increases the size of the focused spot size, d_f, and this has two advantages for thick-section metal cutting. First the larger focused spot size results in a larger depth of focus according to equation (4) and second, the larger focused spot size on the workpiece surface produces a larger kerf width which is essential for thick-section metal cutting using the high-quality fibre laser beam.

However, the propagation of the laser radiation into the metal is also affected by other factors such as extinction coefficient and angle of incidence, which are more favorable for the coupling of the CO_2 laser radiation into the metal workpiece than for the coupling of the fibre laser radiation as long as the initial surface reflection has been overcome. For instance the variation of intensity with depth is given as: $I = I_0 \exp(-4\pi kd/\lambda)$; I_0 is initial intensity, d is the depth, and k the extinction coefficient [**20**]. The extinction coefficient, k, of the 1.06 μm fibre laser radiation is lower than that for the 10.6 μm CO_2 laser radiation. This means that the intensity of the fibre laser radiation falls to $1/e^2$ of the incident value after a shorter distance than for the CO_2 laser radiation and results in a shorter depth of focus for the fibre laser radiation than for the CO_2 laser radiation under similar focusing conditions. The benefits of the angle of incidence on the absorption mechanism of the CO_2 laser beam as compared to the fibre laser beam have also been explained by Mahrle *et al.* [**11**].

5 CONCLUSIONS

Optimization of the laser cutting process parameters – including cutting speed, focal position and focal length – for attainment of a high cut edge quality in the 10 mm stainless steel plate was demonstrated in this study. Dross-free cut edges with lower surface roughness and lower cut edge squareness deviation could be achieved when the cutting speed was reduced from the maximum achievable cutting speed for the used laser power, using the longer focal length lens for focusing the laser beam, and with the focal position located on the bottom workpiece surface as long as the incident power intensity at the workpiece top surface was sufficient to obtain complete penetration of the workpiece. These conditions enhance a high melt removal rate from the cut kerf resulting in a high cut edge quality.

ACKNOWLEDGEMENT

The financial support of the company HT Laser Oy, Finland, towards this research is highly appreciated.

REFERENCES

1 **Ready, J. F.** and **Farson, D. F.** (Eds) Chapter 12: Laser cutting. *LIA handbook of laser materials processing*, 2001, pp. 425–470 (Laser Institute of America).
2 **Hügel, H.** New solid-state lasers and their application potentials. *Optics and Lasers Engng*, 2000, **34**, 213–229.
3 **O'Neill, W., Sparkes, M., Varnham, M., Horley, R., Birch, M., Woods, S.,** and **Harker, A.** High power high brightness industrial fiber laser technology. In Proceedings of the 23rd International Congress on *Applications of lasers and electro optics (ICALEO)*, San Francisco, USA, 4–7 October 2004, paper 301, pp. 1–7 (Laser Institute of America).
4 **Canning, J.** Fibre lasers and related technologies. *Optics and Lasers Engng*, 2006, **44**, 647–676.
5 **Wandera, C.** *Laser cutting of austenitic stainless steel with a high quality laser beam*. Masters Thesis, Lappeenranta University of Technology, Finland, May 2006.
6 **Sparkes, M., Gross, M., Celotto, S., Zhang, T.,** and **O'Neill, W.** Practical and theoretical investigations into inert gas cutting of 304 stainless steel using a high brightness fiber laser. *J. Laser Applic.*, 2008, **20**, 59–67.
7 **Sparkes, M.**, **Gross, M.**, **Celotto, S.**, **Zhang, T.,** and **O'Neill, W.** Inert cutting of medium section stainless steel using a 2.2kW high brightness fibre laser. In Proceeding of the 25th International Congress on *Applications of lasers and electro optics (ICALEO)*, Scottsdale, Arizona, USA, 30 October–2 November 2006, paper 402, pp. 197–205 (Laser Institute of America).
8 **Gross, M. S.**, **Celotto S.** and **O'Neill, W.** Melt flow in narrow thick-section kerfs. In Proceeding of the 25th International Congress on *Applications of lasers and electro optics (ICALEO)*, Scottsdale, Arizona, USA, 30 October–2 November 2006, paper 403, pp. 206–210 (Laser Institute of America).
9 **Himmer, T., Pinder, T., Morgenthal, L.,** and **Beyer, E.** High brightness lasers in cutting applications. In Proceedings of 26th International Congress on *Applications of lasers and electro optics (ICALEO)*, Orlando, Florida, USA, 29 October–1 November 2007, paper 206, pp. 87–91 (Laser Institute of America).
10 **Wandera, C., Kujanpää, V.,** and **Salminen, A.** Laser power requirement for cutting of thick-section steel and effects of processing parameters on mild steel cut quality. *Proc. IMechE, Part B: J. Engineering Manufacture*, 2011, **225**(5), 651–661.
11 **Mahrle, A.**, **Bartels, F.,** and **Beyer, E.** Theoretical aspects of the process efficiency in laser beam cutting with fiber lasers. In Proceedings of 27th International Congress on *Applications of lasers and electro optics (ICALEO)*, Temecula, California, USA, 22–23 October 2008, paper 2006, pp. 703–712 (Laser Institute of America).
12 **Mahrle, A.** and **Beyer, E.** Theoretical aspects of fibre laser cutting. *J. Phys. D: Appl. Phys*, 2009, **42**, 1–9.
13 **Mahrle, A., Lütke, M.,** and **Beyer, E**. Fibre laser cutting: beam absorption characteristics and gas-free remote cutting. *Proc. IMechE, Part C: J. Mechanical Engineering Science*, 2010, **224,** 1007–1018. DOI: 10.1243/09544062JMES1747
14 **Wandera, C., Salminen, A.,** and **Kujanpää, Veli**. Inert gas cutting of thick-section stainless steel and medium-section aluminum using a high power fiber laser. *J. Laser Applic.*, 2009, **21**, 154–161.
15 **Lugan, A.**, **Hilton, P. A.**, and **Taylor, D. W.** The effects of steel composition on the laser cut edge quality of carbon and C-Mn steels. In Proceedings of 21st International Congress on *Applications of lasers and electro optics (ICALEO)*, Scottsdale, Arizona, USA, 14–17 October 2002 (Laser Institute of America).
16 **Olsen, F. O.**, **Hansen, K. S.**, and **Nielsen, J. S.** Multibeam fiber laser cutting. *J. Laser Applic.*, 2009, **21**, 133–138.
17 **Anon.** http://www.outokumpu.com/33392.epibrw (access date 3 June 2010).
18 **Wandera, C.** and **Kujanpää, V.** Characterization of the melt removal rate in laser cutting of thick-section stainless steel. *J. Laser Applic.*, 2010, accepted for publication.
19 **Anon.** *Thermal cutting – classification of thermal cuts. Geometrical product specification and quality tolerances, SFS EN ISO 9013: 2002*. 19 August 2002 (European Committee for Standardization).
20 **Steen, W. M.** Chapter 2: basic laser optics. *Laser material processing*, third edition, 2003, pp. 70–71, and 87 (Springer, New York).

APPENDIX

Notation

BPP	beam parameter product (a measure of beam quality)
d_f	focused spot diameter (minimum beam waist)
D	depth
D_z	beam diameter at distance z from the minimum focused spot
DOF	depth of focus
I	power intensity (I_0 is initial power intensity)
K	the extinction coefficient
M^2	laser beam quality
R_z	mean roughness profile
U	cut edge squareness deviation
z	distance from the minimum focused spot
λ	laser beam wavelength